

Two-level correlation function of critical random matrix ensembles

E. Cuevas

Departamento de Física, Universidad de Murcia, E-30071 Murcia, Spain.

(Dated: February 21, 2019)

The two-level correlation function $R_{d,\beta}(s)$ of d -dimensional disordered models ($d = 1, 2$ and 3) with long-range random hopping amplitudes is investigated numerically at criticality. We focus on models with orthogonal ($\beta = 1$) or unitary ($\beta = 2$) symmetry in the strong ($b^d \ll 1$) coupling regime, where the parameter b^{-d} plays the role of the coupling constant of the model. It is found that $R_{d,\beta}(s)$ is of the form $R_{d,\beta}(s) = 1 + \delta(s) - F_\beta(s^\beta/b^{d\beta})$, where $F_1(x) = \text{erfc}(a_{d,\beta} x)$ and $F_2(x) = \exp(-a_{d,\beta} x^2)$, with $a_{d,\beta}$ being a numerical coefficient depending on the dimensionality and the universality class.

PACS numbers: 71.30.+h, 72.15.Rn, 71.55.Jv, 05.40.-a

I. INTRODUCTION

Random matrix theories are largely and successfully applied in the theoretical description of complex nuclei^{1,2} (where they were first introduced), gauge field theories,^{3,4,5} mesoscopic systems,^{6,7,8,9} and random surfaces in the field of quantum gravity.¹⁰ Their advantage is that it is possible to represent the Hamiltonian of the corresponding system by a large hermitean matrix acting on a finite-dimensional Hilbert space (if one disregards the continuous part of the spectrum).

The random matrices fall into one of three universality classes, named orthogonal ($\beta = 1$), unitary ($\beta = 2$) and symplectic ($\beta = 4$), depending on the global symmetry properties of the Hamiltonian they represent.¹¹ The symmetry parameter β is the number of independent real components that characterizes a matrix element of the Hamiltonian. A system belongs to the orthogonal class if it has both time-reversal and spin-rotation symmetries, to the unitary class if time-reversal symmetry is broken, and to the symplectic class if the system has time-reversal symmetry but spin-rotation is broken. The relevant terms in the Hamiltonian are a coupling to an applied magnetic field, which breaks time-reversal symmetry, and the spin-orbit interaction, which breaks spin-rotation symmetry.

One of the most relevant applications of the random matrix ensembles is to the study of critical phenomena, particularly to the special case of critical statistics which is found at the Anderson metal-insulator transition (MIT) in disordered systems.^{12,13,14,15,16,17,18,19,20,21,22,23,24} At the critical point, the states acquire the property of multifractality, which marks a qualitative difference from the extended states in a metal and localized states in an insulator. These critical states correspond to critical level statistics. Although several ensembles of non-conventional random matrices have been suggested to describe this statistics^{25,26,27,28,29,30,31} we wish to emphasize the power-law random banded matrix model (PRBM),³² for which the multifractality of eigenstates has been rigorously proven.^{32,33} This model is characterized by a variance of their off-diagonal matrix elements, which decay as a power-law with increasing distance from the diagonal. It should be mentioned that all these models are of a one-dimensional nature.

Energy level correlations provide general tools for the statistical description of disordered systems, helping in our understanding of the localization transition. An important statis-

tical measure of spectral correlations is the two-level correlation function (TLCF) of the density of states (DOS), which measures the correlations of the DOS at two different energies. This function has been derived analytically for the PRBM model in the two limiting cases of weak and strong disorder by mapping the corresponding Hamiltonian onto an effective σ -model of a one-dimensional nature³⁴ and using renormalization-group methods,^{35,36} respectively. We stress that, unlike the $1d$ PRBM model, it has not until now been possible to analytically solve the most interesting, from an experimental point of view, disordered models with long-range transfer terms in $d = 2$ and 3 . Thus, explicit results for the TLCF in $2d$ and $3d$ models are still lacking, and finding this function is essential in order to fully understand the MITs. For this reason, we addressed the problem using numerical calculations.

In this work we numerically calculate the TLCF of critical d -dimensional random matrix ensembles with long-range off-diagonal elements and orthogonal or unitary symmetry. Since MITs generically take place at strong disorder (conventional Anderson transition, quantum Hall transition, transition in $d = 2$ for electrons with strong spin-orbit coupling, etc.), we will restrict ourselves to the study of the TLCF in this regime. For the $1d$ case our results are in good agreement, except for the numerical coefficient, with existing analytical estimates.³⁴ In addition, we propose expressions for the TLCF in the $d = 2$ and 3 cases. Apart from the importance of these findings from a general point of view, they may be relevant for several real physical systems (see Sect. II).

The paper begins by first describing the model and the methods used for the calculations in Sec. II. The results for the TLCF in models with orthogonal or unitary symmetry are presented in Sec. III A and III B, respectively. Finally, Sec. IV summarizes our findings.

II. MODEL AND METHODS

In order to fully represent the mesoscopic systems we introduce an explicit dependence on dimensionality d in the widely studied PRBM ensemble.^{32,33,34,37,38,39,40,41,42,43,44,45,46,47,48,49} Thus, we consider a generalization to d dimensions of this ensemble. The corresponding Hamiltonian, which describes non-interacting electrons on a disordered d -dimensional

square lattice with random long-range hopping, is represented by random Hermitean $L^d \times L^d$ matrices $\hat{\mathcal{H}}$ (real for $\beta = 1$ or complex for $\beta = 2$), whose entries are randomly drawn from a normal distribution with zero mean, $\langle \mathcal{H}_{ij} \rangle = 0$, and a variance which depends on the distance between the lattice sites \mathbf{r}_i

$$\langle |\mathcal{H}_{ij}|^2 \rangle = \frac{1}{1 + (|\mathbf{r}_i - \mathbf{r}_j|/b)^{2\alpha}} \times \begin{cases} \frac{1}{2\beta}, & i \neq j \\ \frac{1}{\beta}, & i = j \end{cases}, \quad (1)$$

in which standard Gaussian ensemble normalization is used.⁵⁰

Using field theoretical methods,^{25,32,33,35,37,38,51,52} the PRBM model was shown to undergo a sharp transition at $\alpha = d$ from localized states for $\alpha > d$ to delocalized states for $\alpha < d$. This transition shows all the key features of the Anderson MIT, such as multifractality of the eigenfunctions and non-trivial spectral compressibility at criticality. In what follows, we focus on the critical value $\alpha = d$.

The parameter b^d in Eq. (1) is an effective bandwidth that serves as a continuous control parameter over a whole line of criticality, i.e., for an exponent equal to d in the hopping elements $\mathcal{H}_{ij} \sim b^d$.³⁵ Furthermore, it determines the critical dimensionless conductance in the same way as the dimensionality labels the different Anderson transitions. Each regime is characterized by its respective coupling strength, which depends on the ratio $(\langle |\mathcal{H}_{ii}|^2 \rangle / \langle |\mathcal{H}_{ij}|^2 \rangle)^{1/2} \propto b^{-d}$ between diagonal disorder and the off-diagonal transition matrix elements of the Hamiltonian.⁵³

Many real systems of interest can be described by Hamiltonians (1). Among such systems are optical phonons in disordered dielectric materials coupled by electric dipole forces,⁵⁴ excitations in two-level systems in glasses interacting via elastic strain,⁵⁵ magnetic impurities in metals coupled by an r^{-3} Ruderman-Kittel-Kasuya-Yodida interaction,⁵⁶ and impurity quasiparticle states in two-dimensional disordered d -wave superconductors.⁵⁷ It also describes a particle moving fast through a lattice of Coulomb scatterers with power-law singularity,⁵² the dynamics of two interacting particles in a 1d random potential,⁵⁸ and a quantum chaotic billiard with a non-analytic boundary.⁵⁹

The TLCF is defined in the usual way

$$R_{d,\beta}(\omega) = \frac{1}{\langle \nu(\epsilon) \rangle^2} \langle \nu(\epsilon + \omega/2) \nu(\epsilon - \omega/2) \rangle, \quad (2)$$

where $\nu(\epsilon) = L^{-d} \text{Tr} \delta(\epsilon - \hat{\mathcal{H}})$ is the fluctuating DOS and $\langle \rangle$ denotes averaging over disorder realizations. At the critical point $R_{d,\beta}(\omega)$ acquires a scale-invariant form, if considered as a function of $s = \omega/\Delta$, the frequency normalized to the mean level spacing $\Delta = 1/L^d \langle \nu(\epsilon) \rangle$.^{12,13,14} In the case of constant average DOS, $R_{d,\beta}(s = \omega/\Delta)$ can be simply rewritten as

$$R_{d,\beta}(s) = \delta(s) + \sum_n p(n; s), \quad (3)$$

where $p(n; s)$ is the distribution of distances s_n between n other energy levels and the $\delta(s)$ function describes the self-correlation of the levels.¹¹

The strong disorder limit ($b \ll 1$) of the 1d PRBM model can be studied using the renormalization-group method of Refs. 35 and 36. For orthogonal symmetry, the following result is obtained for the TLCF at the center of the spectral band³⁴

$$R_{1,1}(s) = 1 + \delta(s) - \text{erfc} \left(a_{1,1} \frac{s}{b} \right), \quad (4)$$

where $\text{erfc}(x) = (2/\sqrt{\pi}) \int_x^\infty \exp(-t^2) dt$ is the complementary error function and $a_{1,1} = 1/\sqrt{\pi}$, whereas for unitary symmetry

$$R_{1,2}(s) = 1 + \delta(s) - \exp \left(-a_{1,2} \frac{s^2}{b^2} \right), \quad (5)$$

with $a_{1,2} = 2/\pi$. Notice that for small s , $R_{1,\beta}(s)$ behave as s^β thus reflecting the levels repulsion effect, whereas they tend asymptotically to 1 at large values of s .

For the computation of $R_{d,\beta}(s)$, we unfold the spectrum in each case to a constant density, and rescale it so as to have the mean spacing equal to unity. Then we calculate $p(n; s)$ and use Eq. (3). The system sizes range between $L = 500$ and 6000 in 1d, $L = 20$ and 60 in 2d, and between 8 and 16 in 3d, whereas b^d ranges in the interval $0.02 \leq b^d \leq 0.12$. We consider a small energy window, containing about 10% of the states around the center of the band. The number of random realizations is such that the number of critical levels included for each L is roughly 1.2×10^6 , except for the larger system size in 2d and 3d, for which this number is about 6×10^5 . In order to reduce edge effects, periodic boundary conditions are included.

III. RESULTS

In this section we numerically compute the TLCF $R_{d,\beta}(s)$ of Hamiltonians (1) with the orthogonal or unitary symmetry for different values of the inverse coupling constant $b^d \ll 1$ and various system sizes. We also compare our results with the analytical estimates of Ref. 34 for the 1d model.

A. Orthogonal symmetry

Let us first check the renormalization-group result, Eq. (4), corresponding to the 1d Hamiltonian (1) with orthogonal symmetry $\beta = 1$. The inset of Fig. 1 displays our results for $R_{1,1}(s)$ at different b values for several system sizes: $b = 0.02$, $L = 4000$ (circles), $b = 0.05$, $L = 6000$ (squares), $b = 0.08$, $L = 1000$ (diamonds), $b = 0.1$, $L = 4000$ (up triangles), and $b = 0.12$, $L = 1000$ (left triangles). If the horizontal axis is rescaled by a factor $1/b$ all data should collapse onto a single curve. The main panel of Fig. 1 shows $R_{1,1}(s)$ as a function of the rescaled variable s/b thus confirming the s/b dependence of $R_{1,1}(s)$. The best fit of this data set to Eq. (4) gives the fitting parameter $a_{1,1} = 0.502 \pm 0.003$ which is small than the predicted value $1/\sqrt{\pi} = 0.564$. Ref. 34 reported numerical values of $R_{1,1}(s)$ at $b = 0.1$ for two small

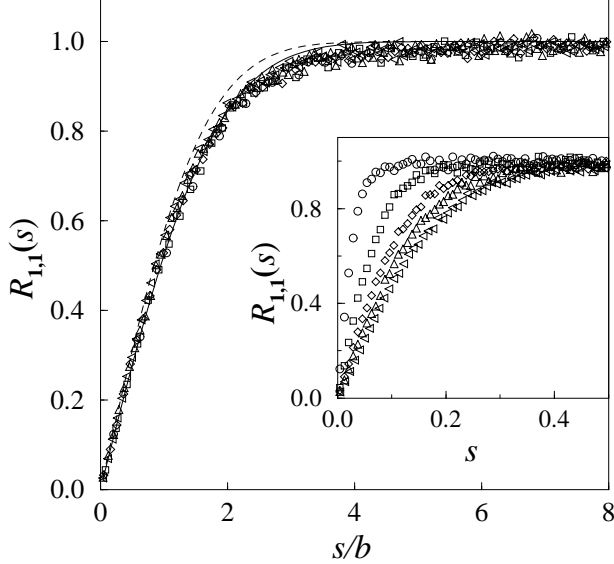


FIG. 1: $R_{1,1}(s)$ for the 1d model (1) with orthogonal symmetry ($\beta = 1$) as a function of the rescaled variable s/b at different b values for several system sizes: $b = 0.02, L = 4000$ (circles), $b = 0.05, L = 6000$ (squares), $b = 0.08, L = 1000$ (diamonds), $b = 0.1, L = 4000$ (up triangles), and $b = 0.12, L = 1000$ (left triangles). The solid and dashed lines represent the renormalization-group estimate, Eq. (4), with the fitting parameter $a_{1,1} = 0.502$ and the predicted $a_{1,1} = 1/\sqrt{\pi}$, respectively. The inset shows the same data on the scale s .

system sizes $L = 256$ and 512 and, as in our calculations, their results were also in relative disagreement with the value $1/\sqrt{\pi}$ in Eq. (4). The solid and dashed lines represent Eq. (4), with the fitting parameter $a_{1,1} = 0.502$ and the predicted $a_{1,1} = 1/\sqrt{\pi}$, respectively. Note that in Ref. 34 a different normalization was used in Eq. (1).

Next we consider the $d = 2$ and 3 cases for which, as mentioned in the Introduction, there are no analytical predictions. The results for $R_{d,1}(s)$ are shown in Fig. 2 in which we were able to collapse both sets of data onto single curves by rescaling the normalized spacing s to the coupling constant $1/b^d$ of the model. Given the similarity of these results with those for the 1d model, a curve of the form

$$R_{d,1}(s) = 1 + \delta(s) - \text{erfc} \left(a_{d,1} \frac{s}{b^d} \right), \quad (6)$$

was fitted to the data points in this graph, and found $a_{2,1} = 0.308 \pm 0.001$ and $a_{3,1} = 0.208 \pm 0.001$. These fits are represented as solid lines in Fig. 2. Thus, the system dimensionality d of the TLCF enters via the inverse coupling constant b^{-d} . We stress that Eq. (6) gives a fairly good fit to the data. The reported data correspond to $b^2 = 0.02, L^2 = 40^2$ (circles), $b^2 = 0.05, L^2 = 20^2$ (squares), $b^2 = 0.08, L^2 = 60^2$ (diamonds), $b^2 = 0.1, L^2 = 20^2$ (up triangles), $b^2 = 0.12, L^2 = 30^2$ (left triangles), $b^3 = 0.02, L^3 = 12^3$ (circles), $b^3 = 0.05, L^3 = 14^3$ (squares), $b^3 = 0.08, L^3 = 12^3$ (diamonds), $b^3 = 0.1, L^3 = 8^3$ (up triangles), and $b^3 = 0.12, L^3 = 10^3$ (left triangles).

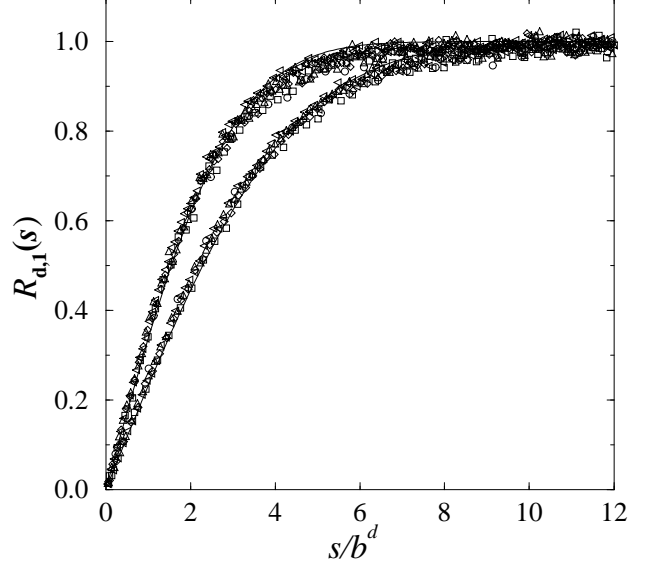


FIG. 2: $R_{d,1}(s)$ for the 2d (upper curve) and 3d (lower curve) models with orthogonal symmetry $\beta = 1$ as a function of the rescaled variable s/b^d at different b^d values for several system sizes: $b^2 = 0.02, L^2 = 40^2$ (circles), $b^2 = 0.05, L^2 = 20^2$ (squares), $b^2 = 0.08, L^2 = 60^2$ (diamonds), $b^2 = 0.1, L^2 = 20^2$ (up triangles), $b^2 = 0.12, L^2 = 30^2$ (left triangles), $b^3 = 0.02, L^3 = 12^3$ (circles), $b^3 = 0.05, L^3 = 14^3$ (squares), $b^3 = 0.08, L^3 = 12^3$ (diamonds), $b^3 = 0.1, L^3 = 8^3$ (up triangles), and $b^3 = 0.12, L^3 = 10^3$ (left triangles). The solid lines are fits to Eq. (6), with the fitting parameters $a_{2,1} = 0.308$ and $a_{3,1} = 0.208$.

(left triangles).

These results allow us to generalize the 1d analytical result, Eq. (4), to the 2d and 3d models by simply replacing the inverse coupling constant b of the 1d case by the corresponding to the d -dimensional case b^d .

The observed b^d dependence of $R_{d,1}(s)$ in Eq. (6) is not surprising since other critical properties, such as the correlation dimension d_2 in 1d and 2d present a similar behavior towards b^d . Specifically, $d_2 = 1 - 1/\pi b$ ($b \gg 1$), and $d_2 = 2b$ ($b \ll 1$) were derived in Refs. 32 and 33 whereas $d_2 = 2 - a_2/b^2$ ($b^2 \gg 1$), and $d_2 = c_2 b^2$ ($b^2 \ll 1$) were numerically found in Ref. 61.

B. Unitary symmetry

As in Sect. III A we first analyze the 1d case in order to compare the numerical data with the analytical result, Eq. (5). Fig. 3 shows $R_{1,2}(s)$ as a function of the rescaled variable s/b . As expected all data points collapse onto the same curve. The inset displays the same data on the s scale. The values of b and L reported are: $b = 0.02, L = 500$ (circles), $b = 0.05, L = 1000$ (squares), $b = 0.08, L = 2000$ (diamonds), $b = 0.1, L = 500$ (up triangles), and $b = 0.12, L = 1000$ (left triangles). Fitting these data to Eq. (5) gives $a_{1,2} = 0.495 \pm 0.005$ which again is small than the predicted

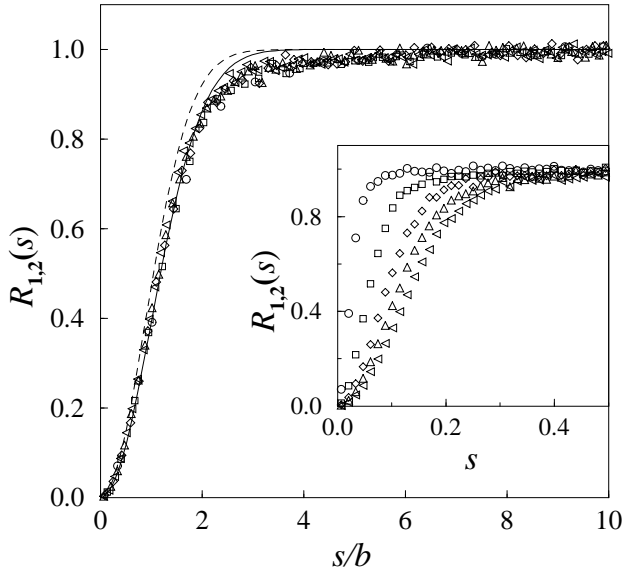


FIG. 3: As in Fig. 1, for the 1d model (1) with unitary symmetry ($\beta = 2$). Data correspond to $b = 0.02, L = 500$ (circles), $b = 0.05, L = 1000$ (squares), $b = 0.08, L = 2000$ (diamonds), $b = 0.1, L = 500$ (up triangles), and $b = 0.12, L = 1000$ (left triangles). The solid and dashed lines represent Eq. (5), with the fitting parameter $a_{1,2} = 0.495$ and the predicted $a_{1,2} = 2/\pi$, respectively. The inset shows the same data on the scale s .

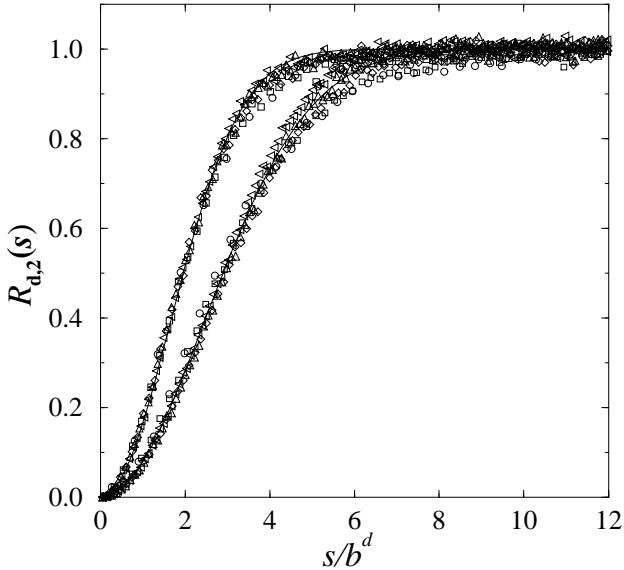


FIG. 4: As in Fig. 2, for the 2d (upper curve) and 3d (lower curve) models with unitary symmetry ($\beta = 2$). Data correspond to $b^2 = 0.02, L^2 = 40^2$ (circles), $b^2 = 0.05, L^2 = 20^2$ (squares), $b^2 = 0.08, L^2 = 60^2$ (diamonds), $b^2 = 0.1, L^2 = 20^2$ (up triangles), $b^2 = 0.12, L^2 = 30^2$ (left triangles), $b^3 = 0.03, L^3 = 12^3$ (circles), $b^3 = 0.05, L^3 = 8^3$ (squares), $b^3 = 0.08, L^3 = 10^3$ (diamonds), $b^3 = 0.1, L^3 = 10^3$ (up triangles), and $b^3 = 0.12, L^3 = 8^3$ (left triangles). The solid lines are fits to Eq. (6), with the fitting parameter $a_{2,2} = 0.181$ and $a_{3,2} = 0.083$, respectively.

TABLE I: The non-universal constants $a_{d,\beta}$ of the TLCF.

	$d = 1$	2	3
$\beta = 1$	0.502	0.308	0.208
2	0.495	0.181	0.083

value $2/\pi = 0.637$. To our knowledge, this is the first numerical confirmation of Eq. (5). The solid and dashed lines represents Eq. (5), with the fitting parameter $a_{1,2} = 0.495$ and the predicted $a_{1,2} = 2/\pi$, respectively.

The results for $R_{d,2}(s)$ in the $d = 2$ and 3 models are shown in Fig. 4, in which one can clearly appreciate the collapse of both sets of data when represented as a function of the rescaled variable s/b^d . As in the cases of $\beta = 1$, a curve of the form

$$R_{d,2}(s) = 1 + \delta(s) - \exp\left(-a_{d,2} \frac{s^2}{b^{2d}}\right), \quad (7)$$

was fitted to the data points in this graph, where $a_{d,\beta}$ is a fitting parameter. The data reported correspond to $b^2 = 0.02, L^2 = 40^2$ (circles), $b^2 = 0.05, L^2 = 20^2$ (squares), $b^2 = 0.08, L^2 = 60^2$ (diamonds), $b^2 = 0.1, L^2 = 20^2$ (up triangles), $b^2 = 0.12, L^2 = 30^2$ (left triangles), $b^3 = 0.03, L^3 = 12^3$ (circles), $b^3 = 0.05, L^3 = 8^3$ (squares), $b^3 = 0.08, L^3 = 10^3$ (diamonds), $b^3 = 0.1, L^3 = 10^3$ (up triangles), and $b^3 = 0.12, L^3 = 8^3$ (left triangles). The solid lines in Fig. 4 are fits to Eq. (7) with fitting parameters $a_{2,2} = 0.181 \pm 0.001$ and $a_{3,2} = 0.083 \pm 0.001$. Note that this equation gives a fairly good fit to the data.

For the system sizes considered ($L^d \gg 1$) we have checked that $R_{d,\beta}(s)$ is an L -independent universal scale-invariant function thus confirming the existence of a critical distribution exactly at the transition. Furthermore, using the nearest-level distribution $p(0; s)$, we verified that the normalized nearest level-variances are indeed scale-invariant at each critical point studied⁶⁰.

Before concluding, we summarize in Table I the non-universal constants $a_{d,\beta}$ found. Note that each value is different for every d and β , thus reflecting its dependence on the Hamiltonian symmetry and dimensionality.

IV. SUMMARY

We present the first numerical results for the two-level correlation function $R_{d,\beta}(s)$ of non-interacting electrons on a d -dimensional disordered system with long-range transfer terms. Models with orthogonal or unitary symmetry at small values of the coupling constant b^{-d} have been considered. The 1d analytical results, Eqs. (4) and (5), are confirmed (except for the numerical constants). We also found that the 1d formulae are valid for the 2d and 3d models if the inverse coupling constant b is replaced by the corresponding to the d -dimensional case, b^d . The proposed Eqs. (6) and (7) are based on numerical results and, at present, should be considered as conjectural. So, further analytical work is needed to check these forms of the TLCF and their origin in the model (1).

Acknowledgments

The author thanks the Spanish DGI for financial support through project number BFM2003-03800.

¹ E.P. Wigner, Ann. Math. **67**, 325 (1958).

² F.J. Dyson, J. Math. Phys. **3**, 140 (1962).

³ J.J.M. Verbaarschot and I. Zahed, Phys. Rev. Lett. **70**, 3852 (1993); J.J.M. Verbaarschot, *ibid.* **72**, 2531 (1994).

⁴ P.W. Brouwer, C. Mudry, B.D. Simons, and A. Altland, Phys. Rev. Lett. **81**, 862 (1998).

⁵ C. Mudry, P.W. Brouwer, and A. Furusaki, Phys. Rev. B **59**, 13221 (1999).

⁶ C.W.J. Beenakker, Rev. Mod. Phys. **69**, 731 (1997).

⁷ Y.V. Fyodorov and H.-J. Sommers, J. Math. Phys. **38**, 1918 (1997).

⁸ T. Guhr, A. Müller-Groeling, and H.A. Weidenmüller, Phys. Rep. **299**, 189 (1998).

⁹ Y. Alhassid, Rev. Mod. Phys. **72**, 895 (2000).

¹⁰ J. Ambjorn, *Fluctuating Geometries in Statistical Mechanics and Field Theory*, Lectures presented at the 1994 Les Houches Summer School.

¹¹ M.L. Mehta, *Random Matrices* (Academic Press, Boston, 1991).

¹² B.L. Altshuler, I.Kh. Zharekeshev, S.A. Kotochigova, and B.I. Shklovskii, Zh. Eksp. Teor. Fiz. **94**, 343 (1988) [Sov. Phys. JETP **67**, 625 (1988)].

¹³ B.I. Shklovskii, B. Shapiro, B.R. Sears, P. Lambrianides, and H.B. Shore, Phys. Rev. B **47**, 11487 (1993).

¹⁴ V.E. Kravtsov, I.V. Lerner, B.L. Altshuler, and A.G. Aronov, Phys. Rev. Lett. **72**, 888 (1994).

¹⁵ B.L. Altshuler and B.I. Shklovskii, Zh. Eksp. Teor. Fiz. **91**, 220 (1986) [Sov. Phys. JETP **64**, 127 (1986)].

¹⁶ A.G. Aronov, V.E. Kravtsov, and I.V. Lerner, Pis'ma Zh. Eksp. Teor. Fiz. **59**, 39 (1994) [JETP Lett. **59**, 40 (1994)]; *ibid*, Phys. Rev. Lett. **74**, 1174 (1995); V.E. Kravtsov and I.V. Lerner, J. Phys. A, **28**, 3623 (1995).

¹⁷ Shinsuke M. Nishigaki, Phys. Rev. E **59**, 2853 (1999).

¹⁸ S.N. Evangelou, Phys. Rev. B **49**, 16805 (1994).

¹⁹ Imre Varga, Etienne Hofstetter, Michael Schreiber, and János Pipek, Phys. Rev. B **52**, 7783 (1995).

²⁰ D. Braun and G. Montambaux, Phys. Rev. B **52**, 13903 (1995).

²¹ B. Grémaud and S.R. Jain, J. Phys. A **31**, L637 (1998).

²² S.R. Jain and A. Khare, Phys. Lett. A **262**, 35 (1999).

²³ E.B. Bogomolny, U. Gerland, and C. Schmit, Phys. Rev. E **59**, R1315 (1999).

²⁴ G. Auberson, S.R. Jain, and A. Khare, J. Phys. A **34**, 695 (2001).

²⁵ V.E. Kravtsov and K.A. Muttalib, Phys. Rev. Lett. **79**, 1913 (1997).

²⁶ Moshe Moshe, Herbert Neuberger, and Boris Shapiro, Phys. Rev. Lett. **73**, 1497 (1994); Jean-Louis Pichard and Boris Shapiro, J. Phys. I France **4**, 623 (1994).

²⁷ K.A. Muttalib, Y. Chen, M.E.H. Ismail, and V.N. Nicopoulos, Phys. Rev. Lett. **71**, 471 (1993).

²⁸ E. Bogomolny, O. Bohigas, J. Keating, and M.P. Plato, Phys. Rev. E **55**, 6707 (1997).

²⁹ A.M. García-García and J.J.M. Verbaarschot, Nuc. Phys. B **586**, 668 (2000).

³⁰ C. Blecken, Y. Chen, and K.A. Muttalib, J. Phys. A **27**, L563 (1994).

³¹ A.M. García-García and J.J.M. Verbaarschot, Phys. Rev. E **67**, 046104 (2003).

³² A.D. Mirlin, Y.V. Fyodorov, F.M. Dittes, J. Quezada, and T.H. Seligman, Phys. Rev. E **54**, 3221 (1996).

³³ A.D. Mirlin, Phys. Rep. **326**, 259 (2000).

³⁴ A.D. Mirlin and F. Evers, Phys. Rev. B **62**, 7920 (2000).

³⁵ L.S. Levitov, Europhys. Lett. **9**, 83 (1989); Phys. Rev. Lett. **64**, 547 (1990).

³⁶ L.S. Levitov, Ann. Phys. (Leipzig) **8**, 697 (1999).

³⁷ F. Evers and A.D. Mirlin, Phys. Rev. Lett. **84**, 3690 (2000).

³⁸ V.E. Kravtsov and A.M. Tsvelik, Phys. Rev. B **62**, 9888 (2000).

³⁹ I. Varga and D. Braun, Phys. Rev. B **61**, R11859 (2000).

⁴⁰ Imre Varga, Phys. Rev. B **66**, 094201 (2002).

⁴¹ E. Cuevas, V. Gasparian, and M. Ortúñ, Phys. Rev. Lett. **87**, 056601 (2001).

⁴² E. Cuevas, M. Ortúñ, V. Gasparian, and A. Pérez-Garrido, Phys. Rev. Lett. **88**, 016401 (2002).

⁴³ E. Cuevas, Phys. Rev. B **66**, 233103 (2002).

⁴⁴ O. Yevtushenko and V.E. Kravtsov, J. Phys. A **36**, 8265 (2003).

⁴⁵ O. Yevtushenko and V.E. Kravtsov, Phys. Rev. E **69**, 026104 (2004).

⁴⁶ E. Cuevas, cond-mat/0310774 (2003).

⁴⁷ A.M. García-García, cond-mat/0306321 (2003).

⁴⁸ E. Cuevas, Phys. Rev. B **68**, 024206 (2003).

⁴⁹ E. Cuevas, Phys. Rev. B **68**, 184206 (2003).

⁵⁰ T.A. Brody, J. Flores, J.B. French, P.A. Mello, A. Pandey, and S.S.M. Wong, Rev. Mod. Phys. **53**, 385 (1981).

⁵¹ V.E. Kravtsov, Ann. Phys. (Leipzig) **8**, 621 (1999).

⁵² B.L. Altshuler and L.S. Levitov, Phys. Rep. **288**, 487 (1997).

⁵³ K.B. Efetov, Adv. Phys. **32**, 53 (1983).

⁵⁴ C.C. Yu, Phys. Rev. Lett. **63**, 1160 (1989).

⁵⁵ R.N. Bhatt and P.A. Lee, Phys. Rev. Lett. **48**, 344 (1982).

⁵⁶ P. Cizeau and J.P. Bouchaud, J. Phys. A **26**, L187 (1993).

⁵⁷ A.V. Balatsky and M.I. Salkola, Phys. Rev. Lett. **76**, 2386 (1996).

⁵⁸ I.V. Ponomarev and P.G. Silvestrov, Phys. Rev. B **56**, 3742 (1997).

⁵⁹ G. Casati and T. Prosen, Physica D **131**, 293 (1999); F. Borgonovi, P. Conti, D. Rebuzzi, B. Hu, and B. Li, *ibid.* **131**, 317 (1999).

⁶⁰ E. Cuevas, Phys. Rev. Lett. **83**, 140 (1999); E. Cuevas, E. Louis, and J.A. Vergés, *ibid.* **77**, 1970 (1996).

⁶¹ E. Cuevas, Phys. Stat. Sol. (b) (to be published).